**Master's Thesis**

# Effects of Buoyancy on Vortices in Laminar n-Butane Diffusion Flame Under Microgravity Condition

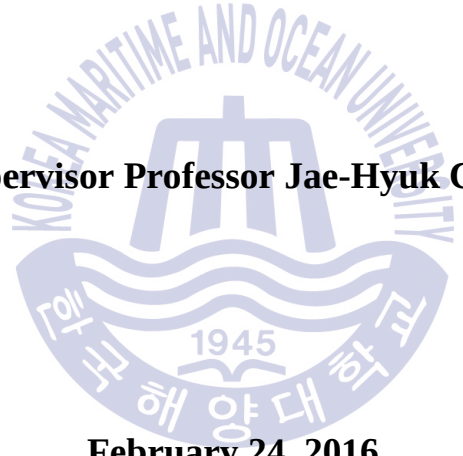


**Supervisor Professor Jae-Hyuk Choi**

**February 24, 2016**

**Department of Marine System Engineering**

**Graduate School of Korea Maritime and Ocean University**

**Thou Ngorn**

본 논문을 넌 투의 공학석사 학위논문으로 인준함.

위원장 윤석훈 (인)

위 원 최재혁 (인)

위 원 박상균 (인)

2016 년 2 월 24 일

한국해양대학교 대학원

**We approved this dissertation submitted by Thou Ngorn for the requirement of Master's Degree of Engineering.**

**Chairman of Supervisory Committee** **Seok-Hun Yoon**  **(Seal)**

**Member of Committee** **Jae-Hyuk Choi**  **(Seal)**

**Member of Committee** **Sang-Kyun Park**  **(Seal)**

**February 24, 2016**

**Graduate School of Korea Maritime and Ocean University**

# Table of Contents

# List of Tables

# List of Figure

# Effects of Buoyancy on Vortices in Laminar n-Butane Diffusion Flame Under Microgravity Condition

Thou Ngorn

Department of Marine System Engineering

Graduate School of Korea Maritime and Ocean University

## Abstract

Flow characteristic, non-buoyancy, laminar jet diffusion flames are described, based on experiments carried out in microgravity condition during 1.5 seconds of dropping from tower. Experimental conditions were conducted in both normal and microgravity condition. Methane ($CH_4$), ethylene ($C_2H_4$) and n-butane ($C_4H_{10}$) fuels were burned in steady air at an ambient temperature and atmospheric pressure. Additionally n-butane flame tests were carried out under microgravity.

Under normal gravity, the experimental study on flow characteristic in various laminar coflow diffusion flames have been conducted with a particular focus on the buoyancy force exerted from gaseous hydrocarbon fuels. Methane, ethylene and n-butane were used as fuels for the experiments. Coflow burner and Schlieren system were used to observe the fuel flow field near nozzle exit and flow characteristics in flames. The result showed that the recirculation zone was appeared near the nozzle exit with the strong negative buoyancy on the fuel stream when burning n-butane which has heavier density than air. As Reynolds

number increases by the control of fuel velocity of n-butane, the vortices were increased and the vortices tips were moved up from the nozzle exit. In addition, it can be found that the heated nozzle can affect the flow fields of fuel stream near the nozzle exit.

Under microgravity condition, the experimental studies on flow characteristic of n-butane flames have been conducted with a particular focus on the non-buoyancy force exerted from gaseous hydrocarbon fuels. The axial velocities of fuel stream were slow up toward the upstream. An indication of absence buoyancy and acceleration due to gravity, the axial velocity were slowly toward the downstream and the particles of fuels stream were not moved in the pockets near the nozzle exit. Therefore, the recirculation zones were disappeared near nozzle exit in n-butane flame under microgravity condition.

**KEY WORDS:** Laminar diffusion flame, n-Butane, Recirculation zone, Fuel flow field, Buoyancy.

## Nomenclature

| | |
|---|---|
| $D$ | Mass diffusivity ($m^2/s$) |
| $d$ | Tube diameter (m) |
| $L_f$ | Flame length (m) |
| $MW$ | Molecular weight (kg/kmol) |
| $Q$ | Volumetric flowrate (m) |
| $\mathrm{Re}$ | Reynolds number |
| $v$ | Velocity (m/s) |
| $x$ | Number of carbon atoms in fuel |
| $y$ | Number of hydrogen atoms in fuel |
| $Y$ | Mass fraction (kg/kg) |
| $R$ | Radius (m) |

### Greek symbols

| | |
|---|---|
| $\mu$ | Dynamic viscosity ($Ns/m^2$) |
| $\upsilon$ | Kinematic viscosity ($m^2/s$) |
| $\rho$ | Density ($kg/m^3$) |
| $\Phi$ | Equivalence ratio |

### Subscripts

| | |
|---|---|
| $A$ | Air |
| $e$ | Exit |
| $f$ | Flame |
| $F$ | Fuel |
| $stoic$ | Stoichiometric |

# Chapter 1 Introduction

Diffusion flames have been the subject of research for many years. The effects of buoyancy and gravity on the burning process have been observed on various studies and these are normally focused on characteristics of fuel stream and flame structure. The objective of this research is to develop an improved understanding of gas jet diffusion flames. The laminar gas jet diffusion flames have been chosen for the study because it is important in all diffusion flame applications such as fires and practical combustion systems. The experiments were carried out under the condition of normal gravity and microgravity resulted in the improvements of understanding the diffusion flame characteristics, buoyancy creation, gravity and burning process.

## 1.1 Backgrounds

Diffusion flames involving convective and diffusive effects are complicated class of combustion process. These include the processes to the reacting flow of fuel stream with air, radiation of flame, chemical kinetics, soot emission, soot formation, diffusion flame, buoyancy and non-buoyancy [1-2].

The flame could be classified into two kinds. One is premixed flame and the other is diffusion flame. The fuel and oxidizer mix before combustion takes place at premixed flame. In case of non-premixed or diffusion flame, the fuel and oxidizer burn as they mix. Premixed and non-premixed flames are subdivided in laminar and turbulent flames. Laminar and turbulent flames are depended on the fuel mass flow [3]. In addition the effects of gravity on the burning process have

been observed from other studies. The influences of the buoyancy on the fuels stream and the combustion processes in laminar diffusion flames were also investigated. The combination of normal gravity and microgravity result would provide the information, both theoretical and experimental, which could improve our understanding of diffusion flames in general and the effects of gravity on the burning process in particular [4].

## 1.2 Objective

The main objective of this study is to understand the buoyancy effect on vortices in laminar n-butane diffusion flame under a microgravity condition. Laminar coflow diffusion flames have been investigated on hydrodynamic structure of hydrocarbon fuels under normal gravity and microgravity condition, taking into account the heavier densities of hydrocarbon gaseous fuel [5]. Dynamic structure of buoyant jet of diffusion flame, heavier fuel density and volumetric expansions were affected the vortex structures [6, 7]. In case of heavier fuel density than air, recirculation zone were appeared near the nozzle exit [5, 8].

According to the reference, buoyancy of diffusion flame could effect to the burnt gas region. Diffusion flames could be inspected between fuel flame zone and oxidized flame zone. The flow fields of hydrodynamic structure in laminar diffusion flame were studied and varying Reynold number effect to flame bulge region and complex vortex effect near nozzle exit were investigated either [9]. We have investigated the flow field near nozzle exit and flame structure with different fuel density by coflow with air. Standard condition of temperature, pressure and normal gravity environment was created in laminar co-flow diffusion flame.

Heated nozzle effect to flow field of near nozzle exit is also investigated. The nozzle absorbs thermal energy from the flame and transfer heat to the fuel stream. Velocity of flow field increases accordingly at the nozzle exit. The nozzle

temperature varies with flame temperature which is caused by different fuel type and different material of nozzle.

## 1.3 Purpose

Laminar diffusion flames are not fully understood and it requires more fundamental studies under normal gravity and under microgravity condition. Through the experiments under microgravity, the effects of buoyancy can be isolated. In this study we focus on characteristic of fuel flow field and characteristic of flame shape in laminar diffusion flame under both normal gravity and microgravity condition.

In this experiment, we investigated the flame structures under the conditions of various fuel velocities and different nozzle temperature. In particular, we concentrated on the recirculation zones in n-butane flame under normal gravity with various Reynold number. Flow field structure of normal coflow diffusion flame with different fuel types and various fuel densities were conducted in both of buoyancy under normal gravity condition and effect of non-buoyancy on vortices under a microgravity condition in laminar n-butane diffusion flames.

# Chapter 2 Literature review of laminar jet diffusion flames

## 2.1 Reacting jet flame physical description

The burning laminar fuel jet has been discussion of the isothermal jet. As the fuel flow along the flame axis, it diffuses radially outward, while the oxidizer (air) diffuses radially inward. The flame surface in nominally defined to exist where the fuel and oxidizer meet in stoichiometric proportions. The equivalence ratio of fuel and oxidizer are consumed at the flame, the equivalence ratio still has meaning sine the products composition relates to a unique value of $\Phi$. The products formed at the flame surface diffuse both radially inward and outward. For an over ventilated flame, there is more than enough oxidizer in the surrounding to continuously burn the fuel. The flame length is simply determined by the axial location when the equivalence ratio [11].

The region where chemical reactions occur is generally quite narrow. As seen in fig. 1, the high temperature reaction zone is an annulus region until the flame tip is reached.

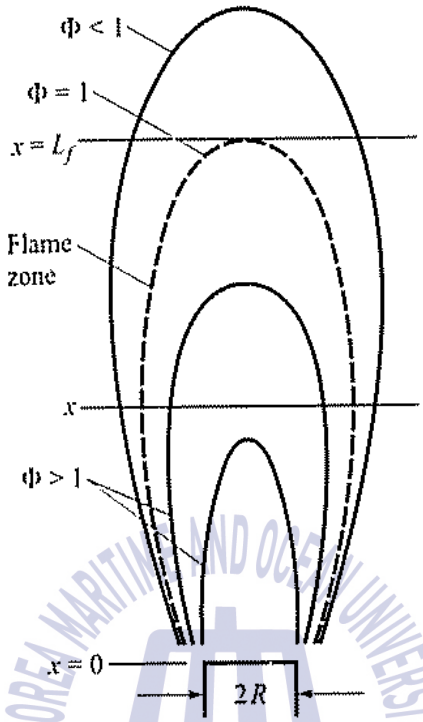


**Fig. 1** Laminar diffusion flame structure [12]

In the upper regions of a vertical flame, there is a sufficient quantity of hot gases that buoyant forces become important. Buoyancy accelerates the flow and cause a narrowing of the flame, since conservation of mass requires streamlines to come closer together as the velocity increases.

For hydrocarbon flames, soot is frequently present, giving the flame its typical orange or yellow appearance. Given sufficient time, soot is formed on the fuel side of the reaction zone and is consumed when it flows into an oxidizing region. Depending on the fuel type and flame residence times, all of the soot that is formed may not be oxidized on its journey through high-temperature oxidizing regions [12].

In this case, soot “wings” may appear, with the soot breaking through the flame. This soot that breaks through is generally referred to as smoke. Fig. 2 show a photograph of an ethylene flame where a soot wing is apparent on the left and right side of the flame tip.

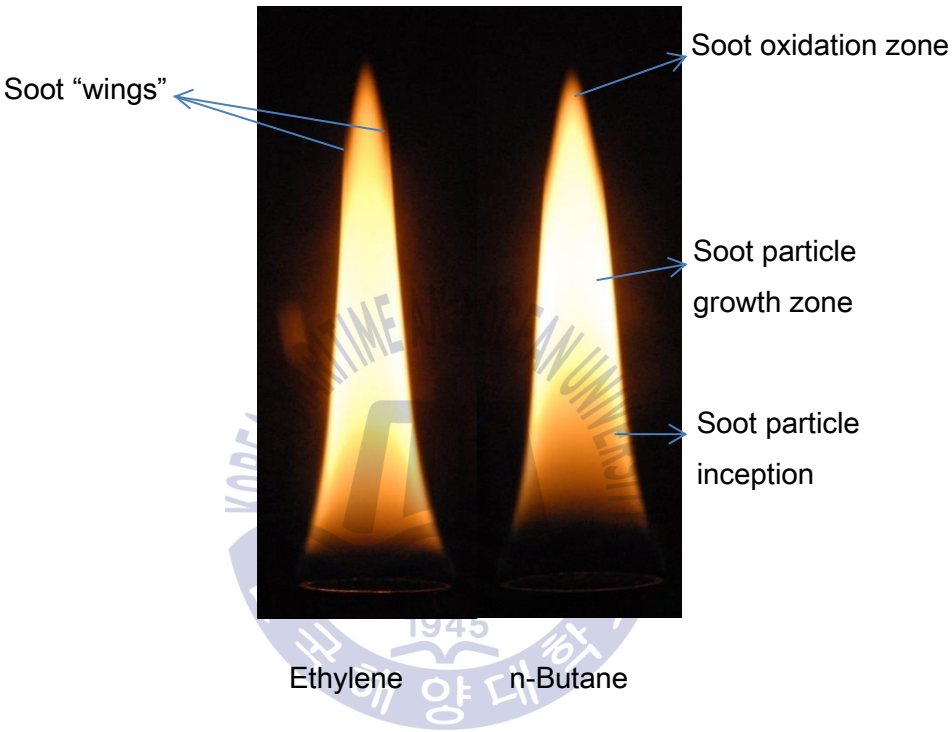


**Fig. 2** Soot formation and destruction zones in laminar jet flames [12]

## 2.2 Flame lengths for circular-port

Laminar jet diffusion flame we wish to highlight has the relationship between flame length and initial conditions. For circular port flames, the flame length does not depend on initial velocity or diameter but, depend on the initial volumetric flowrate. Since the volumetric flowrate ($Q_f$) was various combinations of velocity ($v_e$) and diameter ($R$) of nozzle can yield the same flame length. The flame length is then obtained when radial coordinate equals zero [12].

$$L_f \approx \frac{3}{8\pi}\frac{Q_F}{DY_{F,stoic}} \tag{1}$$

In this equation (1) shows the flame length is indeed proportional to the volumetric flowrate and stoichiometric fuel mass fraction. This implies that fuels that require less air for complete combustion produce shorter flames.

The stoichiometric fuel mass fraction can be calculated as

$$Y_{F,stoic} = \frac{m_F}{m_A + m_F} = \frac{1}{(A/F)_{stoic} + 1} \tag{2}$$

Where

$$(A/F)_{stoic} = (x + (y/4))4.76\frac{MW_A}{MW_F} \tag{3}$$

The volumetric flow rate can be determined as

$$Q_F = v_e \pi R^2 \tag{4}$$

# Chapter 3 Experimental setup

## 3.1 Coflow burner setup

Fig. 3 shows schematics of coflow burner setup. A coflow burner was used in the experiment. The fuel nozzle consisted of a stainless steel tube with an inner diameter of 10.8 mm and a thickness of 1.0 mm, the length of the nozzle was 655 mm to allow the flow of fuel to be in the laminar regime. The coflow tube of transparent acryl cylinder with the inside diameter of 100 mm, 10 mm thickness and 640 mm length. The coflow air was passed through the small glass beads and go through the ceramic honeycomb again to make uniform air flow.

Methane, ethylene and n-butane (purity > 99.5%) were selected as the fuel gaseous. Fuel velocities were 4.45 cm/s for methane, 2.21 cm/s for ethylene. In case of n-butane, fuel velocities vary from 0.54 cm/s to 1.52 cm/s. The air velocities are 3.08~7.19 cm/s. Mass flow controllers were used to control flow rate of hydrocarbon fuel and air.

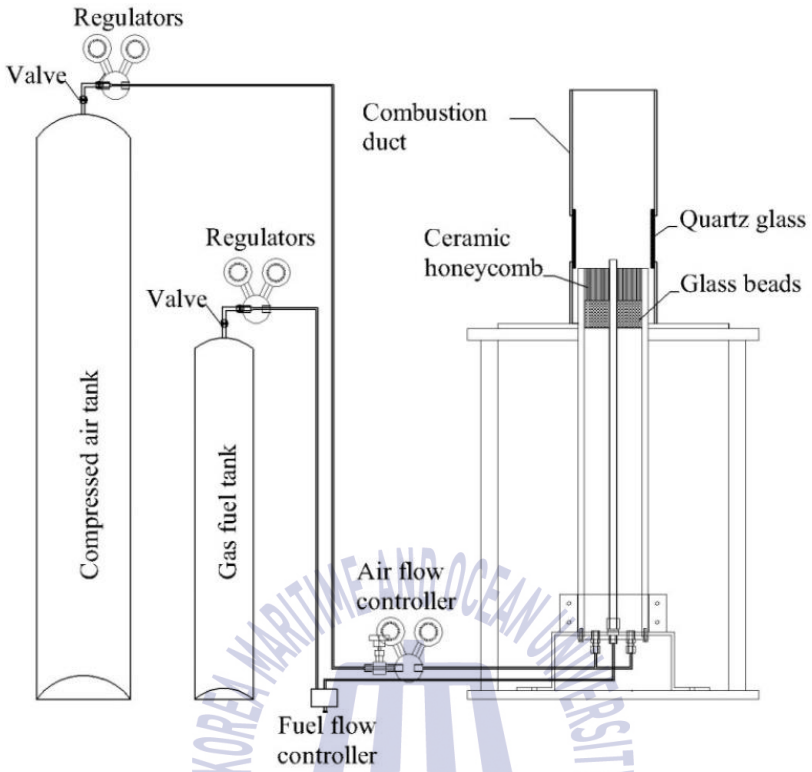


Fig. 3 Schematic of coflow burner setup

## 3.2 Schlieren system

Schlieren system is the system applies for determination of refractive index, wind tunnel research, fluid and air current flow, internal character of glass, flame analysis, sound velocity and the mass of microscopic particles. The brightness variation on the screen will occur according to changes within the medium of the test section [13]. Fig. 4 shows a Schlieren system arrangement, usually employed for flow visualization. The system employed to see the flame structure and observe the flow field in the flame near the nozzle exit in the experiment.

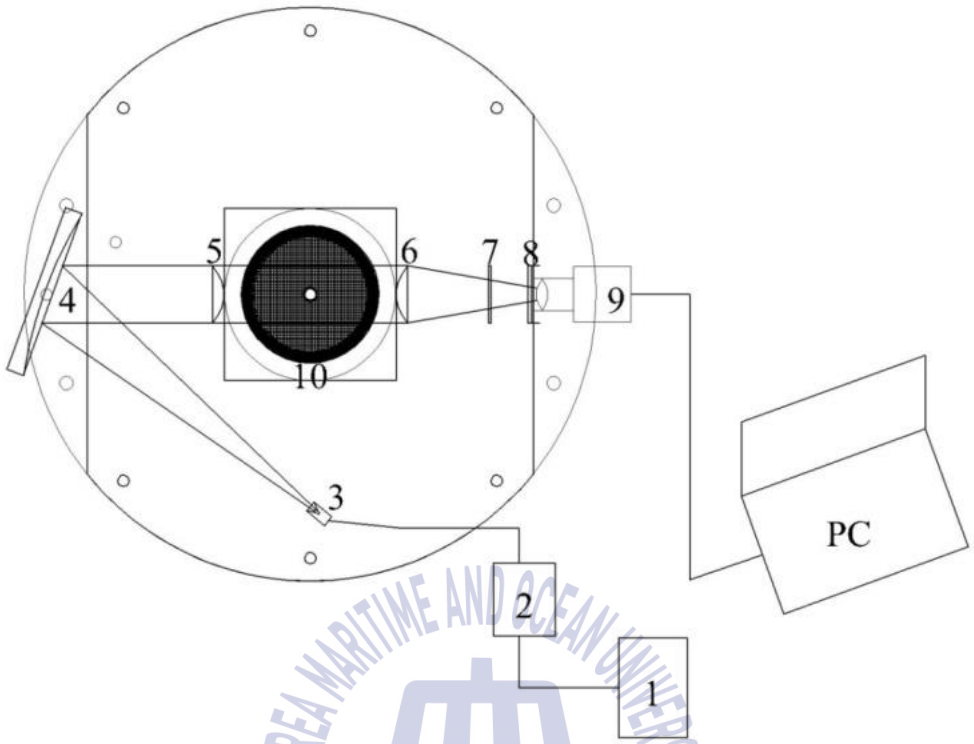


**Fig. 4** Schematic of Schlieren system

**Table 1** Equipment of Schlieren system

| No. | Description |
|---|---|
| 1 | DC 9 V battery |
| 2 | Laser controller |
| 3 | Laser |
| 4 | Parabolic mirror |
| 5 | Plano-convex lens |
| 6 | Plano-convex lens |
| 7 | Absorptive ND filter |
| 8 | Bandpass filter |
| 9 | High speed  camera |


**Fig. 5** Coflow burner and Schlieren system setup under normal gravity

### 3.2.1 Optical components quality requirements

#### Light source

The light source was used a single mode fiber-pigtailed laser and laser diode driver.

#### Parabolic mirror

In the Schlieren system setup we used one parabolic mirror of 150 mm diameter. Focal length of the mirrors about 1.14m and thickness of the mirror glass about 25 mm.

#### Focusing lens

A lens is a transmissivity optical device that affects the focus of a light beam through refraction. This lens is positioned in the Schlieren system in such a way that a flow field is focused on the screen. An ordinary Plano-convex lens can be used [13]. Plano-Convex lenses are optical lenses with the positive focal length and focusing from object to screen or camera.

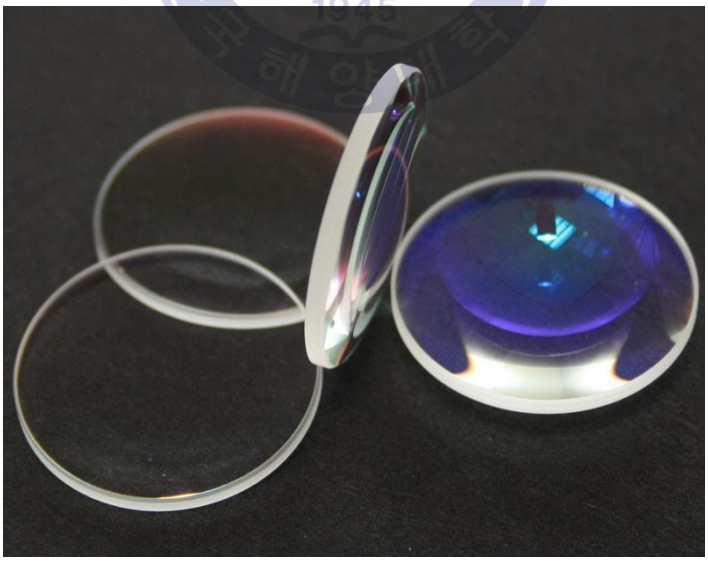

**Fig. 6** Plano-convex lens [13]

Focal length can be calculate as follow

$$\frac{1}{F} = \frac{1}{D_o} + \frac{1}{D_i} \tag{5}$$

Where, $D_o$ : Object to lens distance (m)

$D_i$ : Image to lens distance (m)

F : Focal length of lens (m)

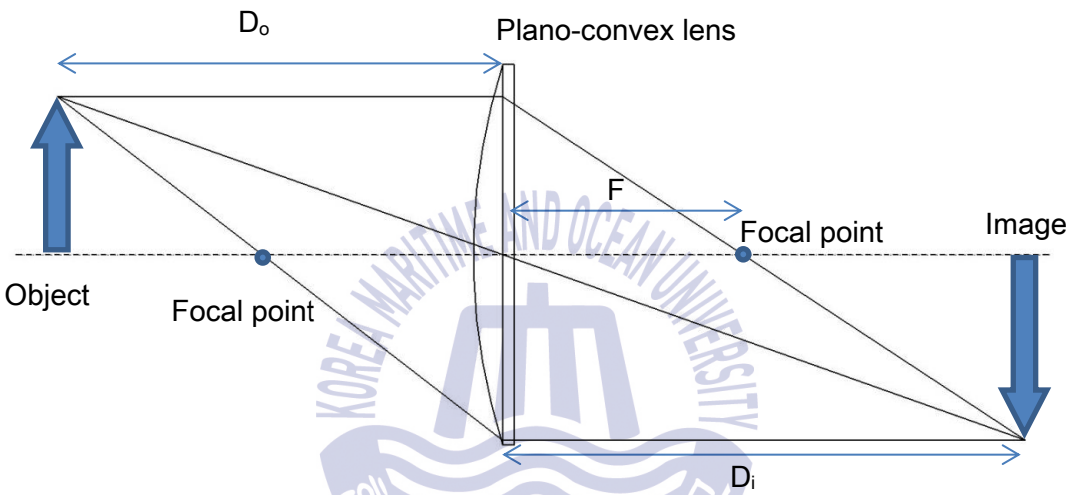


**Fig. 7** Focal length of Plano-convex lens

### Absorptive neutral density filter

These filters possess level spectral transmittance characteristics in the visible region and attenuate light by absorption with minimal reflection. Typically, neutrality and density of absorptive filters are a function of the material and the thickness. Since neutral density filters are held to a specific optical density, the thickness is only a function of the glass type. They are useful in light control applications for measuring instruments and exposure control in imaging. Spectral variations occur as optical density increases [14].


**Fig. 8** Absorptive neutral density filter (optical density from 0.1 to 4.0)

### Bandpass filter

Bandpass filters are widely used in wireless transmitters and receivers. The main function of such a filter in a transmitter is to limit the bandwidth of the output signal to the band allocated for the transmission. This prevents the transmitter from interfering with other stations. In a receiver, a bandpass filter allows signals within a selected range of frequencies to be heard or decoded, while preventing signals at unwanted frequencies from getting through. A bandpass filter also optimizes the signal-to-noise ratio and sensitivity of a receiver [15].


**Fig. 9** Bandpass filter [15]

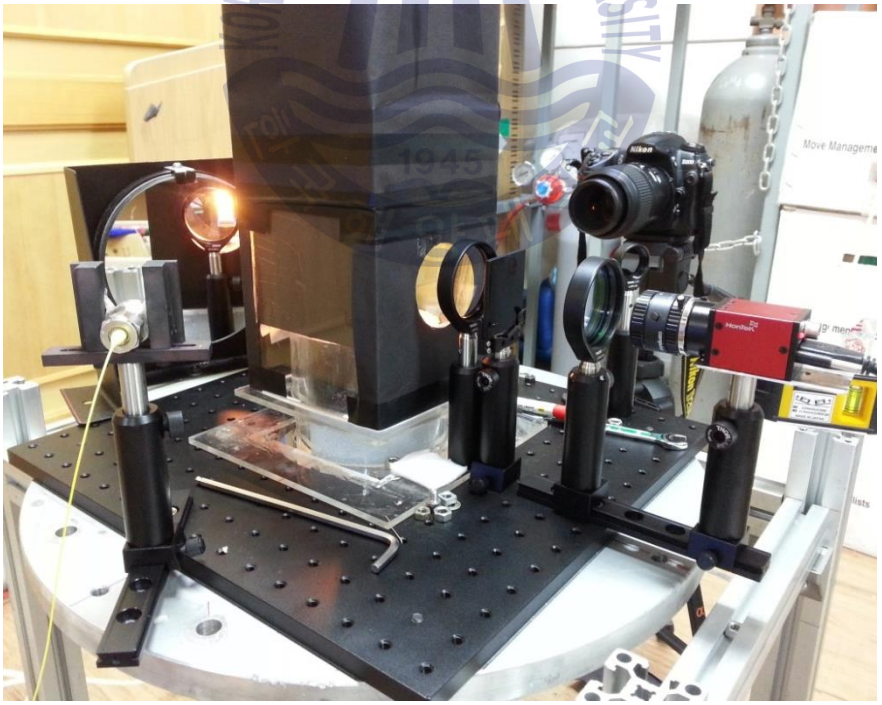

**Fig. 10** Schlieren system setup

### High speed camera

The high speed camera was used to capture image of flame shape and flow field of fuel stream. The camera was used with program setting.

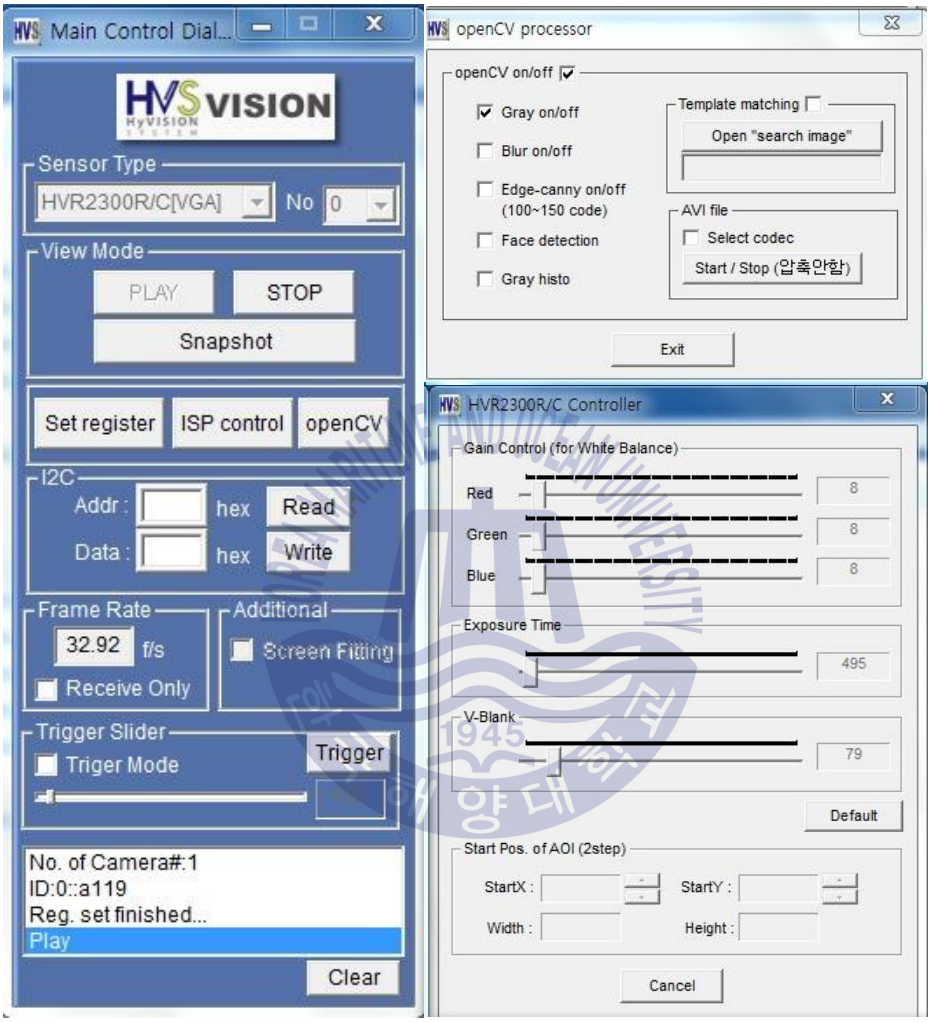


Fig. 11 Camera program setting

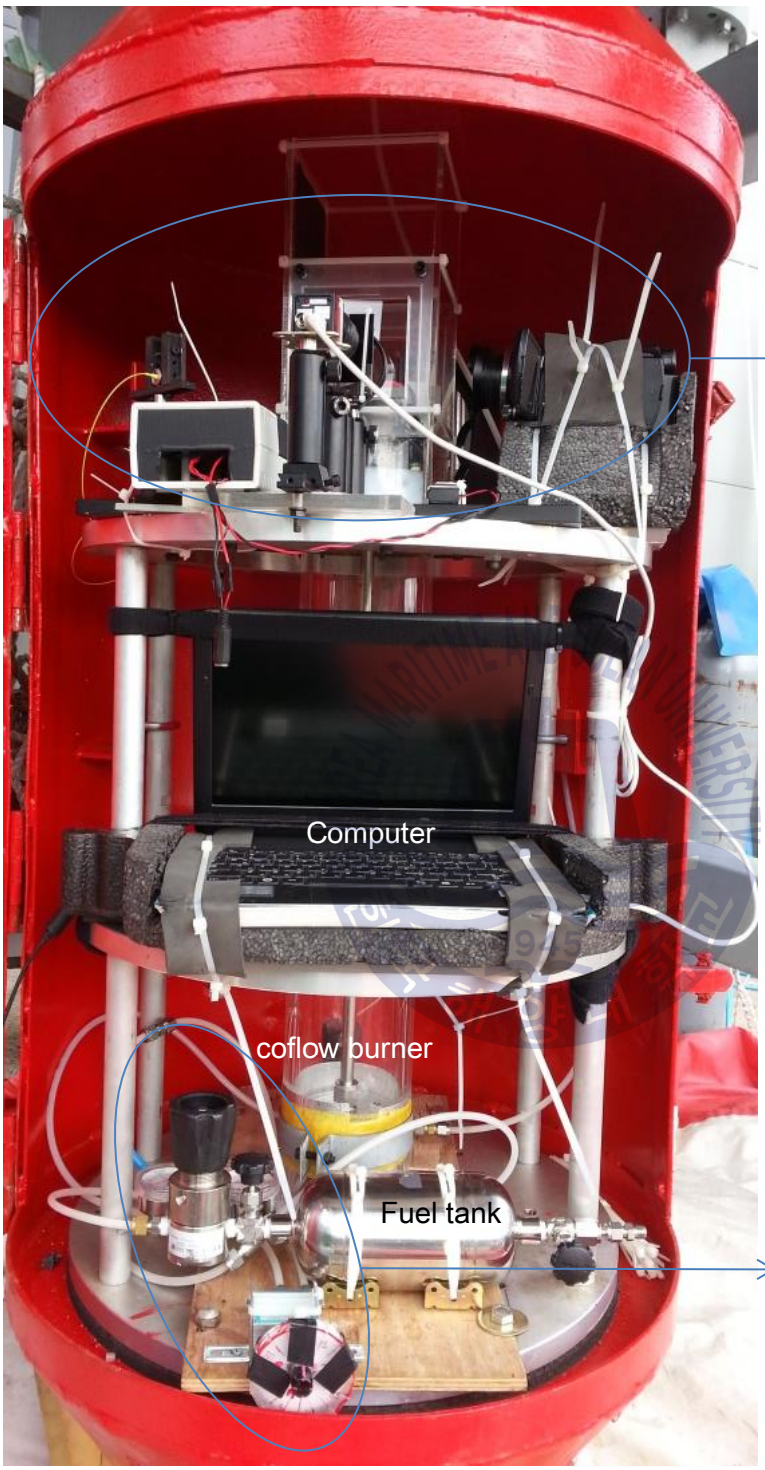


**Fig. 12** Experiment setup in capsules under microgravity condition

### 3.2.2 Microgravity facility of drop tower

There are many different platforms to conducted experiment under microgravity. Microgravity facilities have been conducted such as sounding rocket, parabolic aircraft, space shuttle, international space station and drop tower. While this offers microgravity conditions were extended on cost and time that can develop under microgravity. In this research we used the drop tower to conduct on this experiment. The drop tower offer the best microgravity levels as low as $10^{-6}$g and are the most flexible and adaptable platforms for many scientific experiments.

**Fig. 13** Drop tower experiment

**Fig. 14** Release mechanism system

**Fig. 15** Absorption mechanism system

# Chapter 4 Results and discussion

## 4.1 Under normal gravity condition

### 4.1.1 Laminar diffusion flame structure

Fig. 16 shows the direct flame images for different fuels. Velocities for methane, ethylene and n-butane were 4.43, 2.23 and 1.09 cm/s respectively. Coflow air was supplied with velocity of 6.16 cm/s. The different velocity was selected to keep same flame height as taken in Fig. 16.

In Fig. 16, it can be found that the length for three flames is almost same. For circular-port flames, the flame height does not depend on initial velocity but depend on the initial volumetric flowrate and fuel specification [16]. Different brightness and flame zone structure are caused by different fuel characteristics [17]. For the methane flame structure, the blue zone was higher than ethylene and n-butane flames. For the ethylene flame, blue zone near the nozzle exit was short and luminous zone was smaller than methane and n-butane flame.

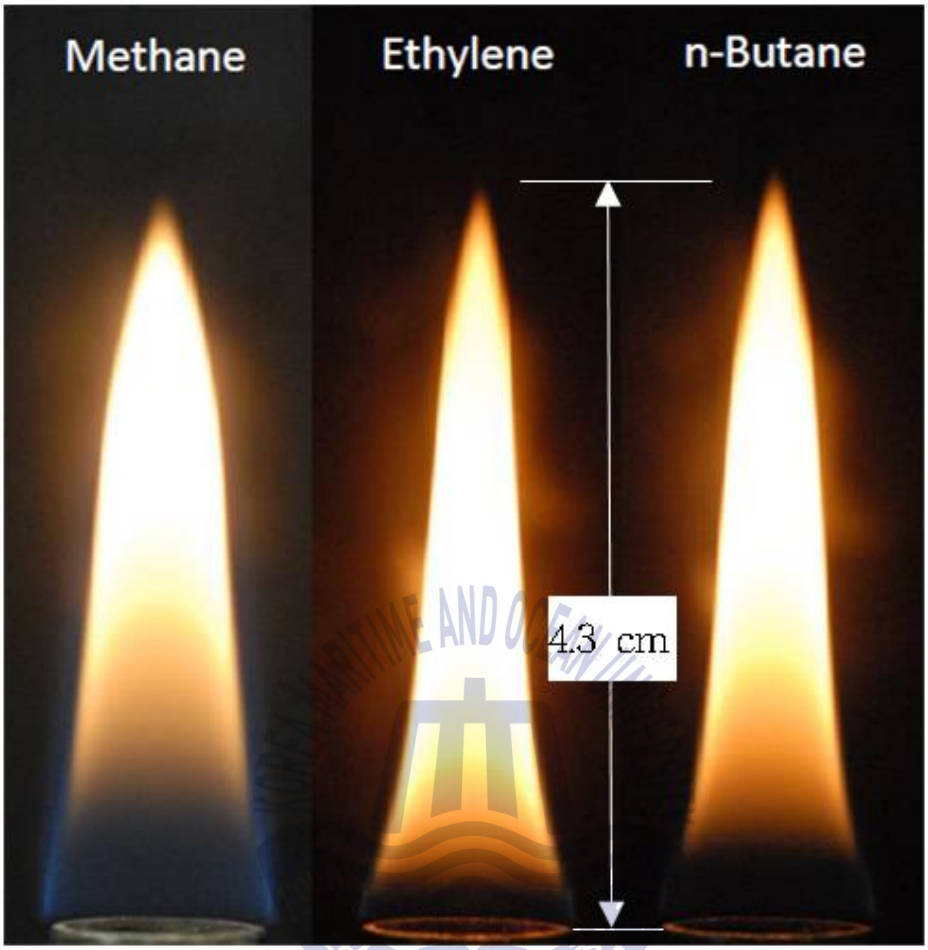


Fig. 16 Direct flame image for different kind of gaseous fuel

In particular, the difference in the brightness is due to sooting characteristic. Methane has less sooting compared with ethylene and n-butane [5]. For the ethane flame structure, the blue zone was higher than ethylene and n-butane flames. Luminous zone of ethylene flame was longer than methane flame and n-butane flame due to the fuel-specific sooting characteristics [18].

### 4.1.2 Flow characteristics

Flow characteristics of methane, ethylene and n-butane laminar diffusion were showed the fuel field of fuels stream with Schlieren image in Fig. 17. Analyzing the flow structure of fuels stream were showed in Fig.18 that all cases of methane, ethylene and n-butane, the path lines are bent towards the centerline due to strong buoyancy effect on the fuels stream. In case of methane and ethane the fuels stream were rapidly reacting with oxidizer to be flames and due to density lighter than air. So methane and ethylene flame were not moved the particle of fuels stream in pocket zone. Especially, n-butane flame, the recirculation zone were appeared near the nozzle exit. Therefore, the strong negative buoyancy force was reacting on the fuels stream and acceleration of the axial velocity toward the downstream. The acceleration of the axial velocity toward the downstream due to density of fuels heavier then air such as n-butane fuel.

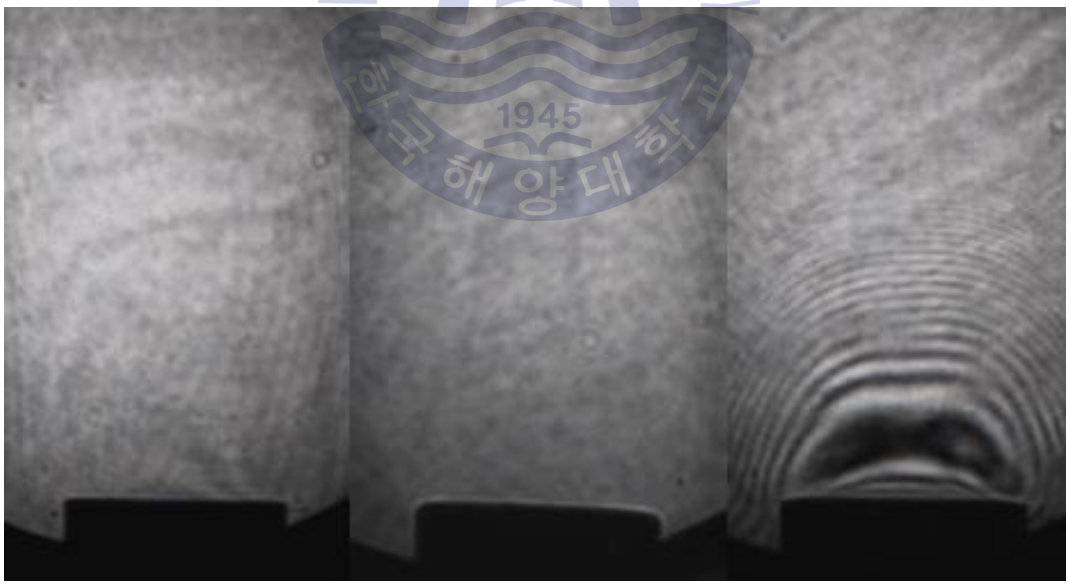

Methane Ethylene n-Butane

**Fig. 17** Visualization of flow field with Schlilieren image for different kind of fuels

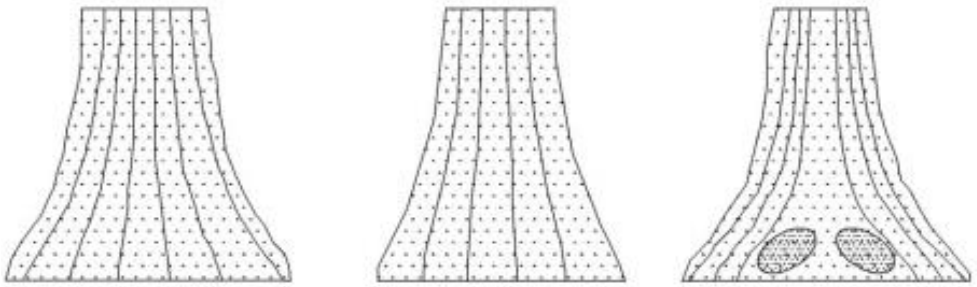

Methane Ethylene n-Butane

**Fig. 18** Path lines flow field of fuels streams by sketch drawing

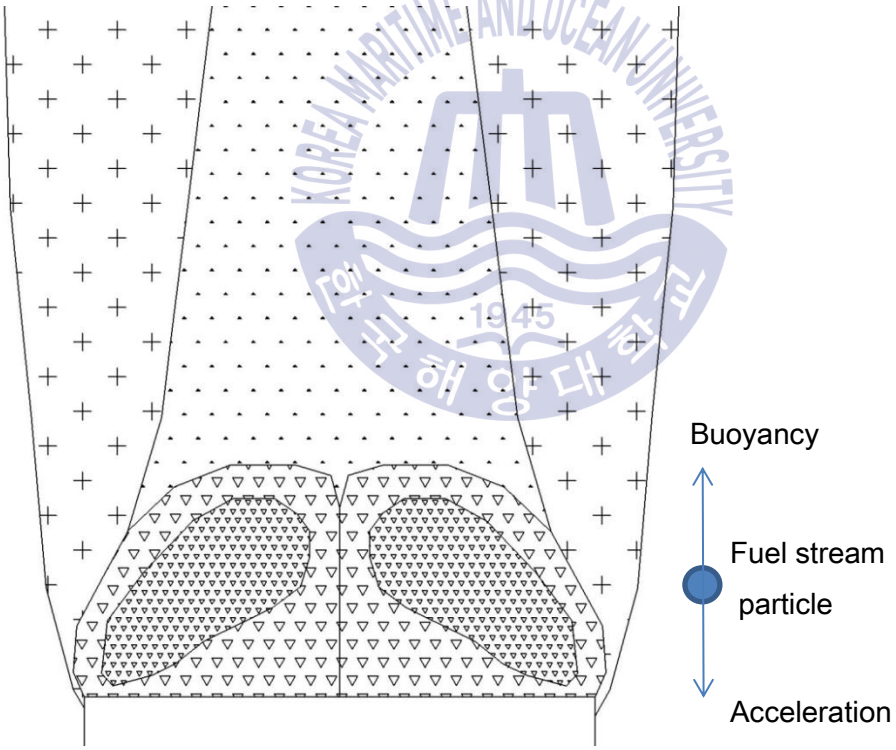


**Fig. 19** Flow field of n-butane flame

### 4.1.3 Effect of heated nozzle to flow field of nozzle exit

The study investigated the effect of the heated nozzle to the flow field near the nozzle exit in coflow diffusion flames. The nozzle absorbs the heat from the flame and transfers the heat to the fuel stream. Therefore, velocity of fuel stream was increased at nozzle exit due to the heated nozzle.

Y. Xiong et al [5] conducted the experiment for three different nozzle conditions. (1) cold flow/cold nozzle, (2) cold flow/ heated nozzle and (3) reacting flow/cold nozzle. They indicated that, in the case of cold flow/cold nozzle, the fuel densities of propane and n-butane were greater than air and buoyancy being directed vertically downwards so the fuel stream rapidly loses their axial momentum and fall down from the nozzle exit. In the case cold flow/heated nozzle, immediately after blowing off the flame, the flow fields had large-scale of vortices near the nozzle exit due to heated nozzle. For the reacting flow/cold nozzle, the recirculation zones were near the nozzle smaller than cold flow/heated nozzle case.

On this experiment, one more experimental case has been derived which is the reacting flow/heated nozzle with the methane, ethylene and n-butane flame showed in Fig. 20 The reacting flow/heated nozzle with n-butane flame shows that the recirculation zone was greater than case of reacting flow/cold nozzle due to fuel velocity increase by reacting with heated nozzle. Nozzle temperature was 156 $^{o}$C measured at 10 mm below the nozzle exit with n-butane as a fuel. The cases of methane and ethylene flames, the fuels stream are rapidly moving up their axial toward the centerline due to the buoyancy and the densities of these fuels being lighter than air. Near the nozzle exit, the fuels streams are not moving in the pocket zone. Therefore, methane and ethylene flames are not appears the recirculation zone near the nozzle exit.

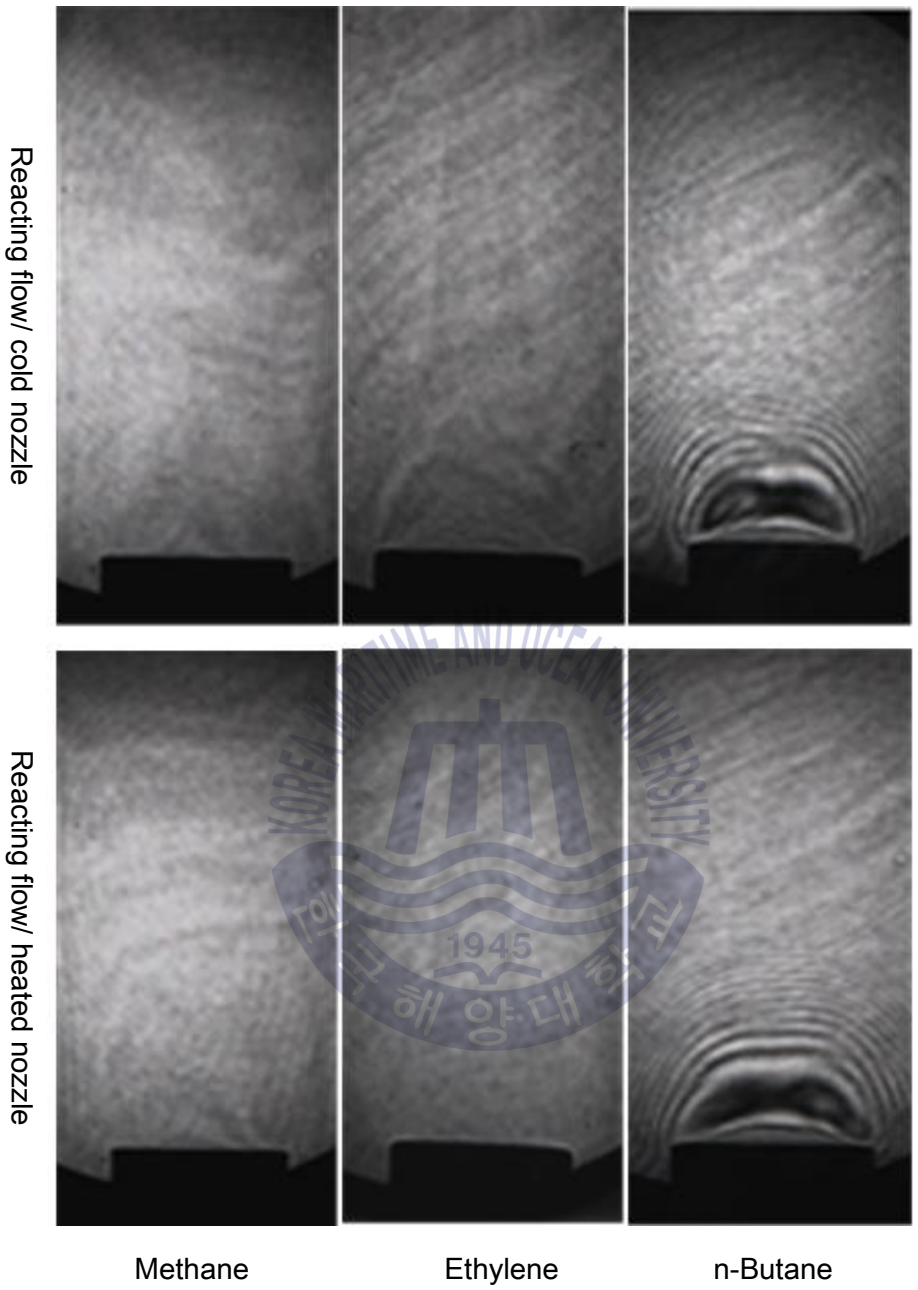


**Fig. 20** Visualization of flow-field with Schilieren image for different kind of fuels

### 4.1.3 Effect of nozzle material properties and fuel type on heated nozzle

Laminar coflow diffusion flame is very sensitive to the fuel type, fuel densities, temperature, pressure and properties of material [19, 21-24]. Gulder et al [25] studied effects of fuel nozzle material properties on soot formation and temperature field in coflow diffusion flame. The results show that the temperature of nozzles was different when they burnt different fuel type (propylene and ethylene), different nozzle material (aluminum, steel and glass) and different local measurement (3 mm and 16.5 mm below the nozzle exit). In case of steel tube with ethylene fuel, the highest nozzle temperature 124 $^{o}$C was measured at 3mm below nozzle exit.

In this study, methane, ethylene and n-butane were burnt with stainless steel tube. Nozzle temperature was measured at 10 mm below nozzle exit. The result showed that the maximum temperatures on burner for methane flame, ethylene flame and n-butane flame are 160 $^{o}$C, 205 $^{o}$C and 156 $^{o}$C respectively. Nozzle temperature of stainless steel tube (205 $^{o}$C) was higher than the steel tube (125 $^{o}$C) with the same Ethylene fuel was supplied. In case of ethylene fuel with the stainless steel nozzle tube, the temperature was higher than another case (aluminum, steel, and glass material whilst burning methane, propylene and n-butane). The Ethylene flame was affected on heated nozzle more than methane flame and n-butane flame. The nozzle material properties have important role as a heat transfer media from flame to the nozzle tube.

**Table 2** Nozzle temperatures measured below 10 mm from the nozzle exit of stainless steel tube

| Hydrocarbon fuel | Nozzle temperature (°C) |
|---|---|
| Methane | 160 |
| Ethylene | 205 |
| n-Butane | 156 |

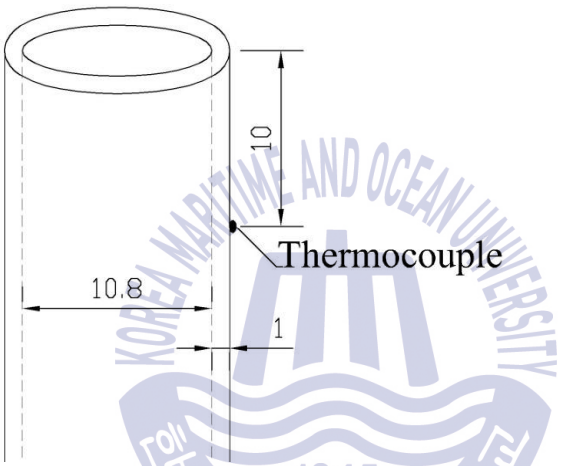


**Fig. 21** Dimension of fuel nozzle tube and location of the thermocouples

### 4.1.4 Effect of Reynold number with various velocities effect on recirculation zone in n-butane flame

Fig. 22 shows the direct flame image for various velocities of n-butane. The flame lengths of laminar diffusion were depended on initial condition. The flame length does depend on stoichiometric fuel mass fraction and volumetric flow of hydrocarbon [11]. For the circular-port flames, the flame lengths were increased due to volumetric flow rat of fuel increased.

Fig. 23 shows the Schlieren images for various velocities of n-butane. Velocity of n-butane to create various Reynolds number on the recirculation zone at the flow field of coflow diffusion flame was varied. The Reynolds number is defined as

$$\mathrm{Re} = \frac{\rho v d}{\mu} \tag{6}$$

Where, $d$ = tube diameter (m)

$v$ = velocity (m/s)

$\rho$ = density (kg/s)

$\mu$ = dynamic viscosity (N-s/m$^2$)

In Equation (6) if the velocity of fuel increases the Reynolds number will be increased. The Reynolds numbers for each flame are 26.8, 33.6, 40.4, 50.7 and 54.3 with various velocities of 0.75, 0.94, 1.13, 1.42 and 1.52 cm/s. Fuel was supplied through the inner nozzle and coflow air velocity was 6.16 cm/s. Fig. 23 shows the increased fuel velocity of n-butane effect on recirculation zone near the nozzle exit.

In case of 0.75 cm/s of fuel velocity, the small vortices were positioned near the nozzle exit. As fuel velocity of n-butane increased up to 0.94, 1.13, 1.42, and

1.52 cm/s, the vortices were greater than that of low velocity. As fuel velocity increased, the centerline was moved up from the nozzle exit and downstream of vortices backward from the centerline. Therefore, recirculation zone become higher and wider with increasing the fuel velocity.

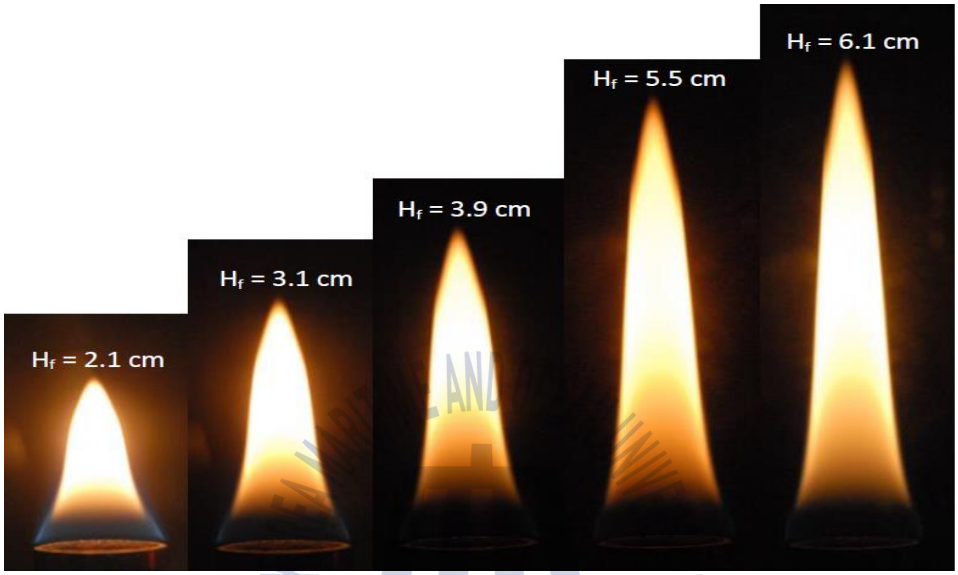


0.75 cm/s 0.94 cm/s 1.13 cm/s 1.42 cm/s 1.52 cm/s

**Fig. 22** Direct flame images for various velocities of n-butane

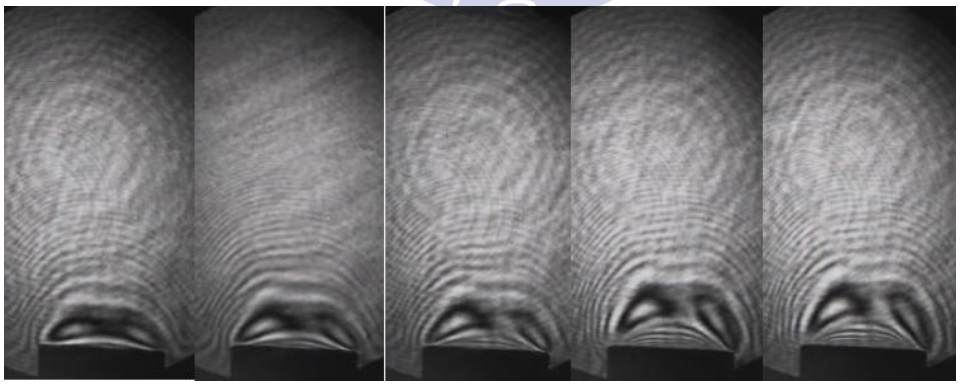

| 0.75cm/s | 0.94cm/s | 1.13cm/s | 1.42cm/s | 1.52cm/s |
|---|---|---|---|---|
| Re=26.8 | Re=33.6 | Re=40.4 | Re=50.7 | Re=54.3 |

**Fig. 23** Schlieren images for various velocities of n-butane

## 4.2 Under microgravity condition

Microgravity investigations are also aimed at understanding the combustion process. A candle flame is an excellent example of the fluid transport mechanisms at worth in the combustion process as it occurs in gravity. The heat produced by the flames melts the wax at the base of the wick. The liquid wax mover closer to the flame it vaporizes and mixes with oxygen at the flame's surface. The products of this chemical reaction are heated and become buoyancy. In microgravity such as burning candle, the virtual absence of gravity driven convection radically changes the appearance of the flame. Without buoyancy driven convection, the flame must rely on the much slower process of diffusion to transport oxygen and fuel vapor [26].

### 4.2.1 Flame characteristics

Laminar diffusion flames of hydrocarbon under microgravity conditions have shown distinct characteristics relative to normal gravity flames [27]. Compared to the flames in normal gravity environments, larger, sootier, and somewhat globular flame are observed in microgravity. This is due to the significant reduction in the buoyancy force, which makes diffusion the dominant mechanism of transport. As a result, increased residence time, enhanced soot formation, radiation cooling due to the larger flame size, and a chemical kinetics limitation on the heat release process are apparently responsible for the very different characteristics of these flames compared to those in normal gravity. In normal gravity environment, laminar diffusion flames of hydrocarbon flicker and are generally yellow, whereas their microgravity counterparts are flicker free, with colors ranging from orange to red to entirely blue, depending on the oxidizer composition [28].

The effect of convection plays a major and different role for different gravitational environments. The partial effect of convection compared to that in

normal gravity, and coupled with the effects of chemistry, radiation and soot formation, results in different flame behaviors under different gravitational levels.

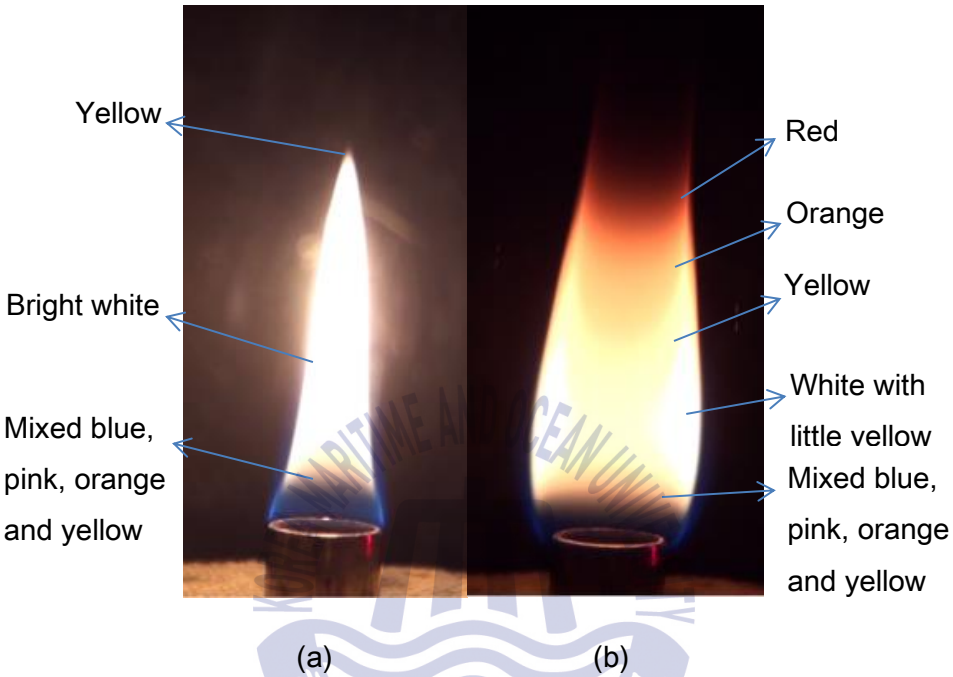


**Fig. 24** (a) Normal gravity and (b) microgravity flames of n-Butane-air at 1 atm, fuel flow rate = 1.07 cm/sec., Air flow rate = 6.16 cm/sec.

Fig. 24 shows an n-butane flame under both normal gravity and microgravity conditions. Compared to the flames in normal gravity environment, longer height and diameter of flame, sootier are observed in microgravity. The flames are taller in microgravity compared to their normal gravity.

### 4.2.2 Flame shapes

Absence of buoyancy and dominance of diffusive processes result in longer residence time, enhanced soot formation, increased radiative loss and cooling by pyrolysis, which are responsible for the observed behavior and characteristics of microgravity flames [29]. Due to the absence of buoyancy inducted acceleration, the axial velocities under microgravity were much lower than under normal gravity. As a result of flow acceleration due to heat release, the velocities were largest in microgravity. The axial velocities in microgravity are much lower and much longer residence time to available for diffusion, thermal radiation and soot surface growth. For diffusion and prolonger residence times are attributed to the enhanced and the flame becomes taller and much wider under microgravity condition. In normal gravity, the flames tips are closed and it changed to open tip in microgravity. These are indicated of OH mass fraction distribution show in Fig. 25.

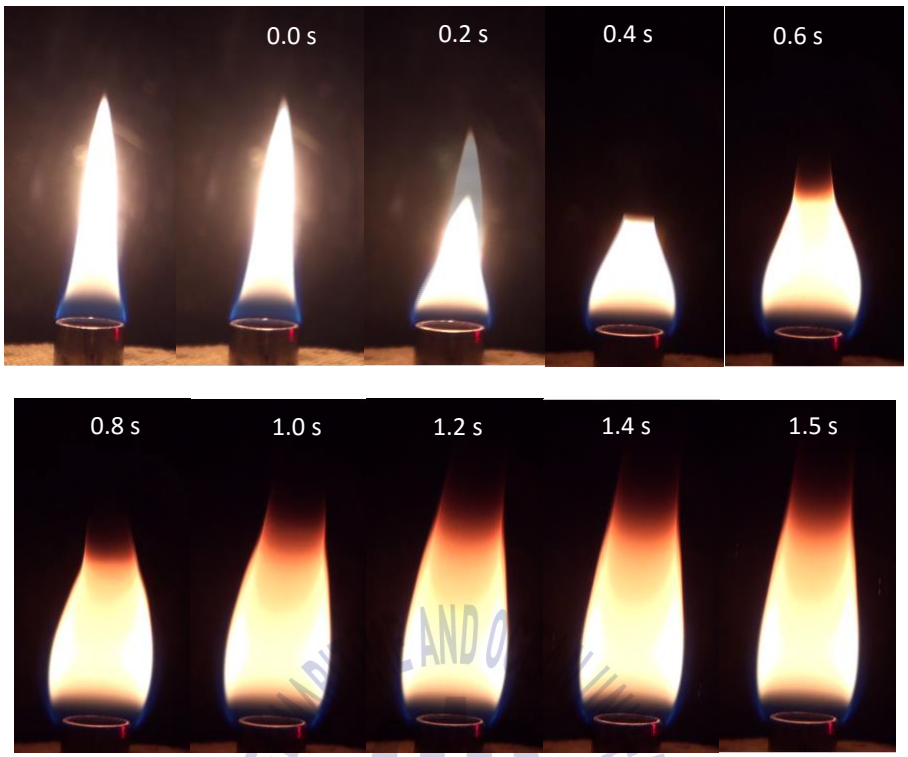


**Fig. 25** Comparison of flames lengths as a function of time for n-butane in microgravity

Although the maximum flame diameter is independent of fuel volume flow rate in both microgravity and normal gravity, the microgravity flames show a fourfold increase in diameter. This is due to the accumulation and slow transport of combustion products in the vicinity of the flame in microgravity.

The transition from a buoyancy controlled flame in normal gravity to momentum controlled flame in microgravity. Fig. 25 shows the flame length from normal to microgravity. First, during 0 to 0.4 seconds the flame length was decreased and then increased from 0.4 to 1.5 seconds.

### 4.2.3 Effect of buoyancy on vortices of n-butane flame under microgravity

The difference between combustion processes in normal gravity and microgravity is due to the absence of buoyancy force. The structure of low diffusion flames are affected by gravity and buoyancy.

Effects of buoyancy on vortices of n-butane flame under microgravity are hard to understand. Therefore, experiments were carried out concerning effects of buoyancy on vortices near nozzle exit. Fig. 26 showed that the absence buoyancy force exerted on the fuel and due to absence gravity the recirculation nozzle was disappeared near nozzle exit.

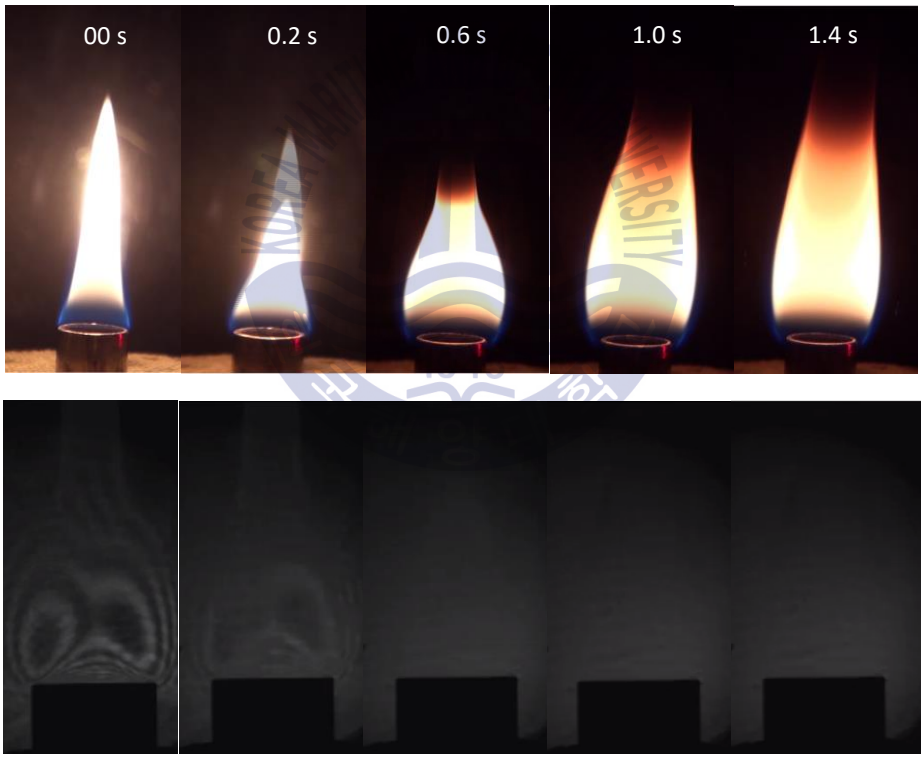


**Fig. 26** Visualization of flow-field with Schilieren image of n-butane flame under both normal and microgravity

# Chapter 5 Conclusion

## 5.1 Under normal gravity

The experiments were carried out under the condition of normal gravity and laminar diffusion flames with different fuels. Methane, ethylene and n-butane were used as fuel gaseous and flow fields near nozzle exit were investigated in the experiment.

Flow characteristics in methane, ethylene and n-butane coflow diffusion flames have been experimentally investigated, accounting for buoyancy effect. Especially, flow field near nozzle exit were investigated. The results can be summarized as follows;

1. According to the experiments of flame structure, flame brightness and flame zone are characterized by the fuel property. Circular-port flame length was dependent on volumetric flow rate and characteristic of hydrocarbon fuel.
2. The vortices were appeared near the nozzle exit with the strong negative buoyancy on the fuel stream because the density of n-butane is heavier than air.
3. Heated nozzle can affect the flow fields of fuel stream near the nozzle exit. The nozzle temperature was varied with fuel type.
4. As Reynolds number increases by the control of velocity, the vortices in n-butane flame become bigger and the vortices tip in n-butane were moved up from the nozzle exit.

## 5.2 Under microgravity condition

Microgravity experiments were carried out at the drop tower for 1.5 seconds. Experimental investigations of buoyancy effect on vortices in laminar diffusion flames under microgravity were made for the following test condition: n-butane burning in steady air supplying, ambient temperature and pressure.

1. Height and diameter of flame in microgravity were longer than in normal gravity.
2. The surface flame shapes are different from normal gravity such as flame zone and color of flame.
3. The recirculation zones were disappeared near the nozzle exit due to absence of buoyancy and gravity.
4. The flame length was decreased during free fall from 0 to 0.4 second and it was increased from 0.4 to 1.5 second.
5. The axial velocities of fuels streams were diverged from the nozzle axis and slowly diffusion toward the upstream under microgravity. Therefore, the absence of buoyancy and gravitational force.
6. The fuel streams were radially outward from the centerline in non-buoyant flames and longer residence time to available for diffusion.

# Reference


[1] C.I.H. Heidelberg “C1-C4 Hydrocarbon Oxidation Mechanism”, Faculty of Chemistry of the Rupertus Carola University of Heidelberg, Germany, 2006.

[2] M.Y. Bahadori, D.P. Stocker, D.F. Vaughan, L. Zhou and R.B. Edelman “Effects of Buoyancy on Laminar, Transitional, and Turbulent Gas Jet Diffusion Flames”, Modern Developments in Energy, Combustion and Spectroscopy , 1993.

[3] J.H. Choi, “Experimental Study on Characteristics of Synergistic Effect of Fuel Mixing on Number Density and Size of soot in Ethylene-base Counterflow Diffusion Flames by Laser Techniques”, Journal of the Korean Society of Marine Engineering, Vol. 33, No. 3, pp. 378~386, 2009.

[4] J.H. Choi and S.K. Park, “A Numerical Study on Soot Formation in Ethylene Diffusion Flame Under 1g and 0g”, Journal of the Korean Society of Marine Engineering, Vol. 37, No. 8, pp. 807~815, 2013.

[5] Y. Xiong, M.S. Cha, and S.H. Chung “Fuel Density Effect on Near Nozzle Flow Field in Small Laminar Coflow Diffusion Flames”, Proc. Combust. Inst. 35 pp. 873-880, 2015.

[6] V.R. Katta, and W.M. Roquemore, “Role of Inner and Outer Structures in Transitional Jet Diffusion Flame”, Combust. Flame 92 pp. 274-282, 1993.

[7] R.W. Davis, E.F. Moore, W.M. Roquemore, L.D. Chen, V. Vilimpoc, and L.P. Goss, “Preliminary Results of a Numerical- Experiment Study of the Dynamic Structure of a Buoyant Jet Diffusion Flame”, Combust. Flame 83 pp. 263–270, 1991.

[8] J. Buckmaster, N. Peters, and Proc. “The Infinite Candle and Its Stability-A Paradigm for Flickering Diffusion Flames”, Combust. Inst. 21 pp. 1829–1836, 1988.

[9] N.A. Eaves, A. Veshkini, C. Riese, Q. Zhang, S.B. Dworkin, and M.J. Thomson, “A Numerical Study of High Pressure, Laminar, Sooting, Ethylene-Air Coflow Diffusion Flames”, Combust. Flame 159 pp. 3179–3190, 2012.

[10] H. Gotoda, Y. Asano, K.H. Chuah G. Kushida, “Nonlinear analysis on Dynamic behavior of Buoyancy-Induced Flame Oscillation Under Swirling Flow” International Journal of Heat and Mass Transfer 52 pp. 5423-5432, 2009.

[11] D. Trees, T.M. Brown, K. Seshadri, M.D. Smooke, G. Balakrishnan, R.W. Pitz, V. Giovangigli, S.P. Nandula, “The Structure of Nonpremixed Hydrogen-Air Flames”Combust. Sci. Technol. 104 pp. 427–439, 1995.

[12] S.R. Turnes. “An Introduction to Combustion Concepts and Applications” McGraw-Hill, USA, 1976.

[13] G.S. Speak, and D.J. Walers, “Optical Considerations and Limitations of the Schlieren Method”, A.R.C. Technical Report R. & M. N. 2859

[14] Edmund Optics, “Schlieren System”, www.edmundoptics.com

[15] Edmund Optics, “Bandpass Filters”, http://www.edmundoptics.com /optics/optical-filters/bandpass-filters.

[16] P.K. Paningrahi and K. Muralidhar, “Laser Schlieren and Shadowgraph” Springer Briefs in Thermal Engineering and Applied Scien, 2012.

[17] F.G. Roper, “The Prediction of Laminar Jet Diffusion Flame Sizes: Part I. Theoretical model”, Combust. Flame 29 pp. 219–234, 1977.

[18] M.R.J. Charest, C.P.T. Groth, and O¨ .L. Gu¨ lder, “A Numerical Study on the Effects of Pressure and Gravity in Laminar Ethylene Diffusion Flames”, Combust. Flame 158 pp. 1933–1945, 2011.

[19] M.A. Mikofski, T.C. williams, C.R. Shaddix and L.G. Blevins, “Flame Height Measurement of Laminar Inverse Diffusion Flames”, Combust. Flame 146 63-72, 2006.

[20] Ö.L. Gülder, “Soot Formation in Laminar Diffusion Flames at Elevated Temperatures”, Combust. Flame 88 pp. 74–82, 1992.

[21] Ö.L. Gülder, “Influence of Sulfur Dioxide on Soot Formation in Diffusion Flames”, Combust. Flame 92 pp. 410–418, 1993.

[22] Ö.L. Gülder, K.A. Thomson, D.R. Snelling, “Effect of Fuel Nozzle Material Properties on Soot Formation and Temperature field in Coflow Laminar Diffusion Flames”, Combust. Flame 144 pp. 426–433, 2006.

[23] E. Rathakrishnan. “Applied Gas Dynamics”, John wiley & Sons (Asia) Pte Ltd, 2010.

[24] A. Datta, “Effects of Gravity on Structure and Entropy Generation of Confined Laminar Diffusion Flames”, International Journal of Thermal Sciences 44 pp. 429-440, 2005.

[25] P.B Sunderland, B.J Mendelson, Z.-G. Yuan and D.L. Urban, “Shapes of Buoyant and Nonbuoyant Laminar Jet Diffusion Flames”, Combustion and Flame 116 pp. 376-386, 1999.

[26] M.Y. Bahadorit, R.B. Edelman, D.P. Stocker, R.G. Sotos and D. F. Voughan, “Effects of Oxygen Concentration on Radiative Loss From Normal Gravity and Microgravity Methane Diffusion Flames” AIAA-92-0243

[27] M.Y. Bahadori and D.P. Stocker “ Oxygen Concentration Effects on

Microgravity Laminar Methane and Propane Diffusion Flames”

[28] D. Zhang, J. Fang, J.F. Guan, J.W. Wang, Y. Zeng, J.J. Wang and Y.M. Zhang, “Laminar Jet Methane/air Diffusion Flame Shapes and Radiation of Low Air Velocity Coflow in Microgravity”, Fuel 130 pp. 25-33, 2014.

[29] M.Y. Bahadori R.B. Edelman R.G. Sotos and D.P. Stocker, “Radiation from Gas-Jet Diffusion Flames in Microgravity Environments”, AIAA-91-0719

[30] F. Liu, G.J. Smallwood and W. Kong, “The importance of thermal radiation transfer in laminar diffusion flames at normal and microgravity”, Journal of Quantitative Spectroscopy & Radiative Transfer 112 pp. 1241-1249, 2011.

# Acknowledgement

Foremost, I would like to express my sincere gratitude to my supervisor, Prof. Jae-Hyuk Choi for his acceptance as my supervisor, his continuous patience, motivation and immense knowledge especially support to study in Korea Maritime and Ocean University.

Second, I would like to thank to Prof. Seok-Hun Yoon and Prof. Sang-Kyun Park for their valuable suggestions and comments on my thesis.

Third, I would never forget to encouragement from Prof. Kwon-Hae Cho and all professors in department of Marine System Engineering, who have taught me the courses.

Fourth, I would like to express my gratitude to Mr. Sehyun Jang for his guidance me and comments on my thesis. And I would like also to thank to my laboratory members for their kindness to help to do experiments. In addition, I would like to thank the assistance of Department of Marine System Engineering and assistance in many areas, for their support and guidance me to achieve the project.

Furthermore, I would also like to thank to Prof. Seol Hyeon Park and his lab members from department of Mechanical system and automobile engineering of Chosun University for their guidance and kindness to help me setup the Schlieren system.

And finally, I would like to express my deepest gratitude to my parents and my sisters who supported everything to me.